

The ITER Baseline Scenario at ASDEX Upgrade and TCV

T. Pütterich¹, O. Sauter², F. Bagnato², V. Bobkov¹, Y. Camenen³, S. Coda², M.G. Dunne¹,
 F. Eriksson⁴, E. Fable¹, R. Fischer¹, E. Fransson⁴, A. Karpushov², B. Labit², P.T Lang¹,
 A. Merle², R.M. McDermott¹, Ph. Neubert¹, W. Suttrop¹, M. Vallar², I. Voitsekhovitch⁵,
 F. Widmer³, M. Willensdorfer¹, the EUROFUSION MST1 TEAM⁶, the TCV Team⁷
 and the ASDEX Upgrade Team⁸

¹Max-Planck-Institut für Plasmaphysik, D-85748 Garching, Germany

²École Polytechnique Fédérale de Lausanne (EPFL), Swiss Plasma Center (SPC), Switzerland

³CNRS, Aix-Marseille Univ., PIIM UMR7345 Marseille, France

⁴Chalmers University of Technology Gothenburg, Sweden

⁵EURATOM/CCFE Fusion Association, Culham Science Centre Abingdon OX14 3DB, UK

⁶See author list of “B. Labit et al 2019 Nucl. Fusion 59086020”

⁷See author list of “S. Coda et al 2019 Nucl. Fusion 59112023”

⁸See author list of “H. Meyer et al. 2019 Nucl. Fusion 59 112014”

Investigations of the ITER baseline scenario (BLS) either match the dimensionless parameters of ITER such as the safety factor $q_{95} = 3$, normalized plasma pressure $\beta_N = 1.8$, plasma-shape parameters (e.g. elongation κ or triangularity δ), Greenwald fraction $f_{GW} = 0.85$, collisionality $\nu^* \approx 0.01$, or they mimic operational strategies envisaged for the BLS in ITER. The goal is to identify important physics ingredients, which then must be understood and extrapolated to the full scale plasma in ITER via physics models. Using this strategy, possible showstoppers, models shortcomings and important physics can be identified and verified.

A possible issue identified in the past at ASDEX Upgrade (AUG) is that for operation at low q_{95} and strong shaping, i.e. $\delta > 0.3$, large pedestal pressures and densities with ELMs are observed [1], which are beyond the ITER allowed sizes and extend even beyond the multi-machine ELM size scaling [2]. For similar strongly shaped plasmas, at TCV, the observations are very similar and high densities and large ELMs are also observed [3]. Another issue identified at AUG with W-walls, is that the normalized H-mode confinement is approximately 15 % too low ($H_{98,(y,2)} \approx 0.85$) for the appropriate ITER relevant $\beta_N \approx 1.8$, i.e. for obtaining ITER-relevant stored energies more heating power is needed than the scaling predicts. As examples with ($H_{98,(y,2)} \approx 1.0$) exist in the C-wall AUG, it was attempted to regain the confinement via N-seeding in the W-wall AUG. However, for the ITER BLS no confinement improvement via N-seeding was observed [4]. A deeper analysis and a comparison to the ITER BLS at TCV is presented in the following.

In figure 1(a), the evaluation of $H_{98,(y,2)}$ is plotted versus β_N for highly shaped discharges in H-mode. For the high-density discharges with Greenwald fraction $f_{GW} > 0.55$ the blue

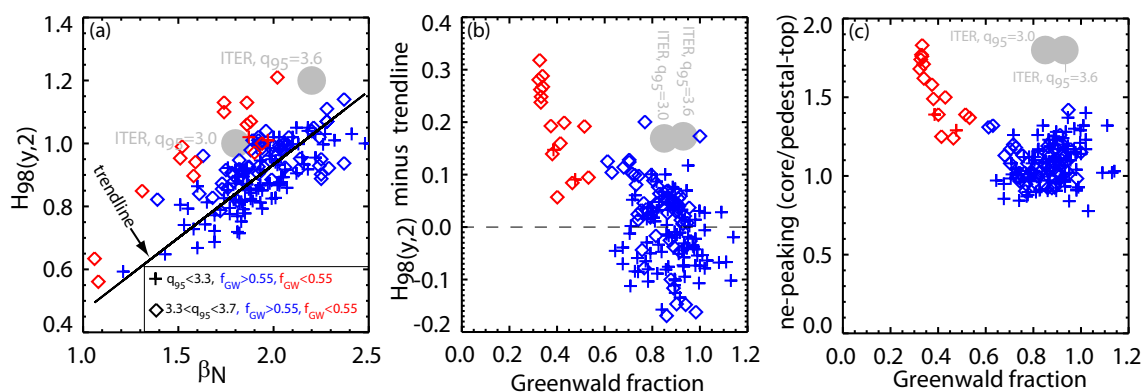


Fig. 1: Trends in global parameters for the ITER BLS discharges in AUG. More details in the text.

crosses ($3.0 < q_{95} < 3.3$) indicate a clear trend, which is described by the black trendline, i.e. $H_{98,(y,2)} = 0.467 \cdot \beta_N$. The data is parallel shifted to the actual goal for baseline discharges in ITER ($q_{95} = 3$) indicated by the left gray circle. A suggestion to achieve the ITER goals, i.e. the same fusion power, for lower plasma current ($q_{95} \approx 3.6$) and thus improved operational and mode stability, is investigated in discharges corresponding to the blue diamonds. However, these data follow approximately the same trendline. The corresponding goal in the depicted parameters which are also indicated in the right gray circle is also not achieved in AUG. Only discharges with $f_{GW} < 0.55$ (red crosses for $3.0 < q_{95} < 3.3$ and red diamonds for $3.3 < q_{95} < 3.7$) manage to appear above the trendline indicating correspondence with the ITER goals in $H_{98,(y,2)}$ for $\beta_N \approx 1.8$. Still, the ITER $f_{GW} = 0.85$ is not met. The low density branch is only accessible in AUG if magnetic perturbations are applied which then lead to density pump-out [5]. As for all scenarios the data arrange parallel to the trendline, i.e. for higher β_N higher $H_{98,(y,2)}$ are achieved, the deviation of the $H_{98,(y,2)}$ values from the trendline is investigated versus f_{GW} in figure 1(b). A clear dependence of f_{GW} becomes apparent, which corresponds mostly to electron density n_e , as the plasma current and shapes of all data points in the database are very similar. Note an improved performance at low densities is a general observation (e.g. in [6]) from various machines. For the presented database also density peaking is very closely linked to the f_{GW} as can be seen in figure 1(c).

Note, that the underlying physics is related to collisionality [7]. It is not clear to what extent density peaking is the underlying reason for the systematically improved $H_{98,(y,2)}$, as for the investigations in [6] other players such as ExB-shear, turbulence stabilization via fast particles and a dependence on heating distribution between electrons and ions are under discussion. However, it is worthwhile to note that for discharges in TCV, where all of the above play a minor role the $H_{98,(y,2)}$ -factors are above 1 at $\beta_N = 1.8$, while also a β_N dependence is observed [3]. In figure 2, the density profiles of a typical ITER BLS in TCV is compared to one from AUG. Even though the TCV case exhibits a larger collisionality than the AUG case, the density profile is strongly peaked, which via an ASTRA-GLF23 modeling is found to be caused by the specifics of the here dominant ITG turbulence and partly also by the particle source of the neutral beam heating [3]. For AUG, the modeling of the profiles using ASTRA-TGLF [8, 9] is presented in figure 3(a) along with a low density case in figure 3(b). TGLF is used to predict all presented profiles within $\rho_{tor} = 0.85$, while the boundary condition at $\rho_{tor} = 0.85$ is taken from the experimental data. The modeled profiles are consistent with the experimental data in all cases and specifically the density peaking at low density is reproduced quantitatively. Note, that for the high-density case a scan of the core radiated power was performed by changing the W-concentration from 0 to 6E-5, while all profiles are remarkably stiff considering that core radiation is scanned in the model from 0 to 2.8 MW, for 7 MW of transported power at the edge. The experimental value for the core radiation, i.e. 1.4 MW,

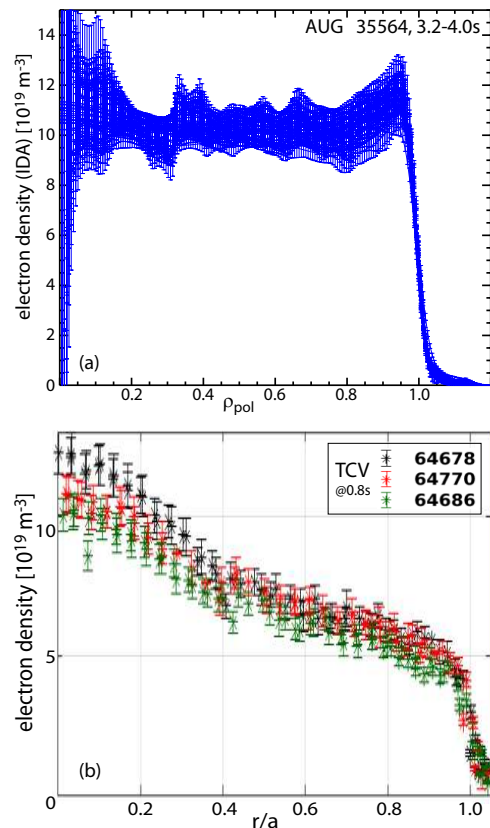


Fig. 2: Comparison of typical density profiles from ITER BLS in TCV and AUG.

is covered by this scan. For the high densities, the heat fluxes equilibrate quickly such that core radiation can be well associated with missing heating power and thus, the radiated power should correspond to a case in which the respective heating power is not injected and no core radiation exists. The analysis presented in figure 3(a) suggests that all profiles would be almost

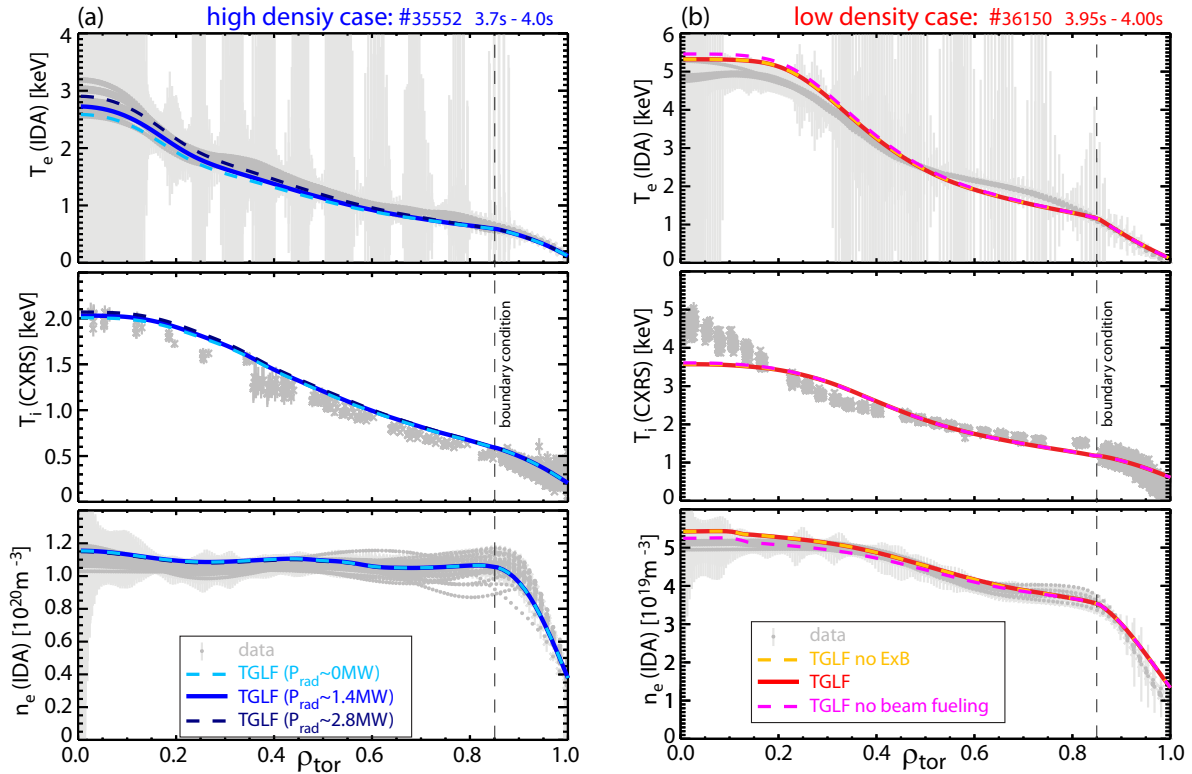


Fig. 3: Modeling of core profiles using TGLF for a high- and low-density case. More details in the text.

unchanged for lower heating power and thus, β_N should not change, while $H_{98,(y,2)}$ would increase as radiation losses are not considered for it. However, in experiment, a decrease of heating power is associated with a change of β_N . For the above high-density case a change of 2MW beam heating relates to β_N change of about 0.2-0.4 as can be judged from comparable discharges. Considering the good agreement of the core modeling and its insensitivity to core radiation, this change must originate from the pedestal and thus, cannot be investigated with the presented modeling. Note, that at very small heating powers just above the LH-threshold (≈ 3 -4 MW) small ELMs help to obtain quasi-stable discharges with positive deviations from the trendline for $H_{98,(y,2)}$ (in figure 1(a)). For such a scenario an additional core radiation of 2.8 MW will most probably make a difference.

For the low collisionality case in figure 3(b) the influence of ExB shear was found to be negligible for the core profiles, while the beam fueling is observed to have only a very minor effect consistent with earlier results from AUG [7]. Thus, the experimental observations indicate that the density peaking is a natural consequence of the density change. It should be noted that in $H_{98,(y,2)}$ a positive density behavior is assumed, i.e. $H_{98,(y,2)} \propto n_e^{0.41}$, which expresses a co-linearity of good energy and particle confinement, but is problematic when describing scenarios with particularly high densities due to high shaping or gas fueling. Thus, a new confinement scaling [10] was developed in the framework of ITPA focusing also on high-density discharges and in particularly the discharges with strong shaping like the ITER BLS.

This new scaling (here called H20IL), which corresponds to the ITER-like scaling in [10] gives $H20IL \propto n_e^{0.147}$. Reproducing figure 1(a) and 1(b) using H20IL instead of $H_{98,(y,2)}$ results in figure 4(a) and 4(b). Clearly, figure 4(a) still exhibits a dependence of H20IL on β_N , i.e. heating power. The trendline ($H20IL = 0.5 \cdot \beta_N$) is 0.9 at $\beta_N = 1.8$, but there are many

data points also at $H20IL=1$, which corresponds to the expected behavior according to the scaling. However, the scaling predicts for ITER about 25% too low confinement such that the ITER value has to be $H20IL=1.25$ in order for ITER to fulfill its design value. This value is not reached with any of the data points in the AUG database. Furthermore the changed density dependence of H20IL leads to the observations that low density data points do not perform better anymore such that also the data points with density peaking do not exceed the trendline sufficiently, as can be seen in figure 4(b). It may be speculated that the changed density scaling in H20IL takes the effect of density peaking into account and projects this effect onto density. For ITER, it is well known that high densities are consistent with low collisionalities and thus strong density peaking. This combination is not abundant in the AUG database and at least less abundant in the ITPA database used for the development of H20IL.

Conclusions The AUG and TCV strongly shaped plasmas at $q_{95} < 3.7$ behave very similar in terms of the large low-frequent ELMs and the high natural densities. It is observed that at TCV a strong density peaking is the natural result of turbulent transport and beam fueling even at high collisionalities, while at AUG the density peaking is only observed at low collisionalities, consistent with earlier observations. A deficiency of the confinement in terms of $H_{98,(y,2)}$ is observed at AUG, but vanishes for low density cases featuring density peaking at AUG. The $H_{98,(y,2)}$ at TCV shows no deficiencies and for all cases density peaking is observed in agreement with ASTRA GLF23 modelling. When judging the confinement with the newly developed ITPA20-IL scaling the density peaking plays no role for AUG and $H20IL=1$ can be obtained in the ITER BLS at AUG, however, the ITPA20-IL scaling predicts too small performance for ITER itself. Possibly density peaking, which will occur in ITER at high densities is neglected in this scaling which would help closing the performance gap for ITER.

References

- | | |
|--|--|
| [1] J. Schweinzer <i>et al.</i> , NF 56 , 106007 (2016) | [2] A. Loarte <i>et al.</i> , PPCF 45 , 1549 (2003) |
| [3] O. Sauter <i>et al.</i> , 28th IAEA FEC (2020), EX/P4-18 | [4] T. Pütterich <i>et al.</i> , 27th IAEA FEC (2018), EX/P8-4 |
| [5] N. Leuthold <i>et al.</i> , PPCF 59 , 055004 (2017) | [6] A. Sips <i>et al.</i> , NF 58 , 126010 (2018) |
| [7] C. Angioni <i>et al.</i> , PPCF 51 , 124017 (2009) | [8] E. Fable <i>et al.</i> , PPCF 55 , 124028 (2013) |
| [9] G. M. Staebler <i>et al.</i> , PoP 23 , 062518 (2016) | [10] G. Verdoolaege <i>et al.</i> , NF 61 , 076006 (2021) |

Acknowledgement This work has been carried out within the framework of the EUROfusion Consortium and has received funding from the Euratom research and training programme 2014-2018 and 2019-2020 under grant agreement No 633053. The views and opinions expressed herein do not necessarily reflect those of the European Commission. This work was supported in part by the Swiss National Science Foundation.

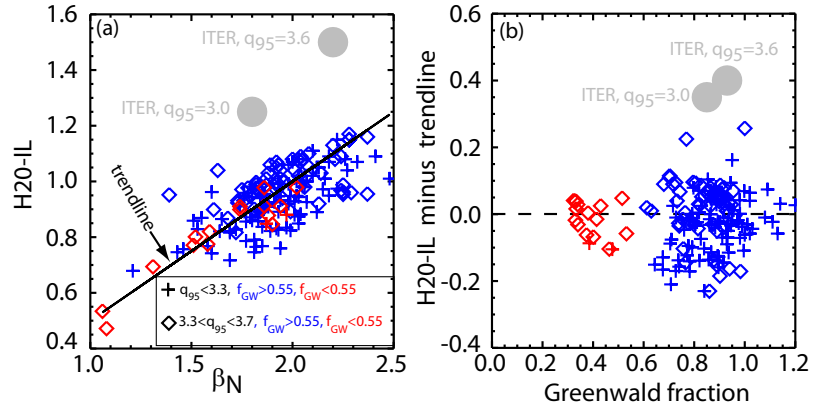


Fig. 2: Corresponding to figure 1(a) and (b) but using the new ITPA20-IL [10] scaling instead of $H_{98,(y,2)}$